

Evaluation of the seismic performance of off-centre bracing system with ductile element in steel frames

Mohammad Bazzaz*, Ali Kheyroddin, Mohammad Ali Kafi and Zahra Andalib

Faculty of Civil Engineering, Semnan University, Semnan, Iran

(Received April 02, 2011, Revised October 12, 2011, Accepted March 26, 2012)

Abstract. In order to evaluate the dynamic behavior of passive energy dissipation system, two steps need to be considered for prediction of structural response in the presence of ductile element in an off-centre bracing system. The first is a detailed analysis of the proposed ductile element and the second is the effect of this ductile element on an off-centre bracing system. The use of ductile bracing system is expanding in steel structures in order to increase the force reduction factor. Therefore, regarding the nonlinear behavior of steel material used in an off-centre bracing systems and using ductile element in OBS bracing systems, the seismic evaluation of the mentioned systems seems to be necessary. This paper aims to study linear and nonlinear behavior of steel frames with off-centre bracing system and ductile element, in order to get the best position of these bracing elements. To achieve this purpose, the modeling has been done with ANSYS software. The optimum eccentricity has been obtained by modeling three steel frames with different eccentricities and evaluating the results of them. The analytical results showed that the model OBS-C with 0.3 eccentricities has higher performance among the models.

Keywords: finite elements; nonlinear analysis; off-centre bracing; ductile element; cyclic load; steel structure.

1. Introduction

Passive energy dissipation systems are supplemental energy dissipation mechanisms added to a structure in order to improve its seismic performance (Murthy 2005, Andalib *et al.* 2010). Several comprehensive references are available on the behavior, analysis, and design of passive systems (e.g., Ibrahim *et al.* 2007, Marshall *et al.* 2010, Hanson *et al.* 2001). With designated energy dissipative devices installed in a structure, a large portion of the input energy supplied by earthquake can be dissipated; hence the damage to the parent structure is minimized (Chan Ricky *et al.* 2008).

Concerning the hazardous earthquake which may cause financial damage or in some cases loss of life, finding a new way for the dissipation of damaging energy of earthquake is very important. Traditionally, steel bracing system has been used to increase the lateral load resistance of steel structures. Steel moment resisting frame structures possess high strength and significant ductility, thus are effective structural forms for earthquake-resistant designs (Kim *et al.* 2002, Lee *et al.* 2005). However, the load carrying efficiency of such designs is limited when an earthquake induces large story drift because of the lower structural stiffness of the steel frames (Hsu *et al.* 2011). In recent years, the

* Corresponding author, Mr., E-mail: M_Bazzaz@sun.semnan.ac.ir

concept of steel bracing has also been applied to the retrofitting of reinforced concrete frames (Maheri *et al.* 2008). Braced structures with concentric braces are among earthquake resistant systems widely used in frames with joint connections (Kafi 2008). Using centric braces only in structures with the height of 50m is permissible (Building and Housing Research Center 2007). Therefore using these braces is very common because of high stiffness, the ease of implementation and low cost of them. Despite the benefits mentioned limited ductility of concentric braces, however, caused poor functionality against earthquake. To solve this problem, using frictional connections (Mualla *et al.* 2002), covering jacket and ductile element in bracing systems have been proposed (Bazzaz *et al.* 2011). Therefore, in this paper new bracing system with dissipative circular element which has more ductility has been evaluated.

2. Review of the latest researches

Extensive research on the toggle-brace damper system has been conducted by earlier researcher (Constantinou *et al.* 2001). An off-centre bracing system consists basically of the non-straight tension strut BOC with an eccentricity designated as “ e ” is shown in Fig. 1. The mid-point O is connected to the corner by the third member AO . Once the load is applied, all these three members are stretched and, therefore, act in tension. As the load increases, the original geometry changes and a new formulation of equilibrium equations, based on the new geometry, is required. Hence the characteristics of such an off-centre system are geometrically nonlinear (Moghaddam *et al.* 1999). And another investigation revealed that the degree of nonlinearity depends mainly on the amount of eccentricity and the relative stiffness of the third bracing member, in this paper embedded ductile element in the third member of off-centre bracing systems (AO), and it is clear that stiffness of this system is lower than the system without ductile element. The purpose of this system is mainly on the dissipation of energy attention to achieve stiffness results of previous research (Moghaddam *et al.* 1995). Genetic algorithms on the optimal size and location of dampers have been presented (Singh *et al.* 2002), and also other comprehensive investigations on the buckling and damping in y-braced and X-braced frame have been done (Majidzamani *et al.* 2006, 2011).

As it mentioned above in order to evaluate the dynamic behavior of passive energy dissipation system, two steps need to be taken into account to predict the structural response in the presence of ductile element in an off-centre bracing system. The first step is analyzing of proposed ductile element, earlier researchers worked on a ductile element and gained valuable results (e.g., Tabatabaei 2007, Beheshti 2008, Hizji 2008). To achieve the high performance of this new system a ductile element that acts as a bending fuse proposed in the previous research (Kafi 2008) has been used to act as a first defensive system.

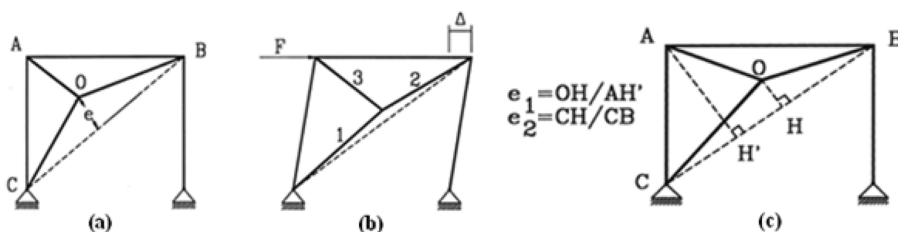


Fig. 1 Off-centre bracing system. (a) Undeformed, (b) Deformed, (c) Eccentricity parameters e_1 and e_2

3. Geometrical specification of frame with off-centre brace and ductile element

In order to investigate the optimum position of ductile element in an off-centre brace frame, a single-story, single-bay hinged frame with off-centre figuration and ductile element in member AO (member AO shown in Fig. 1) has been analyzed and studied. The model for simplification has been named (OBS-C). From this model three different figurations have been created. The variation of these three models is in value of e_1 , So that three models were called OBS-C0.2, OBS-C0.3 and OBS-C0.4. The numerals revealed the value of eccentricity e_1 by taking $e_2 = 0.5$ in all of them. Concerning the geometry of models, the length of three members of off-centre brace frame calculated and the specifications of frames are shown in Table 1. The sections of profiles are two channels at a distance of 20 mm from each other. Space between columns' filler and brace member is 380 mm and the thickness of fillers and plates of corner connections are 20 mm. Connections modeled as pin assuming that pin joint is more conservative. The models are shown in Fig. 2.

Circular element is modeled taking external diameter 220 mm, thickness 12 mm and length of 200 mm. To design steel elements, AISC-ASD (American Institute of Steel Construction 2005) code is used and to calculate seismic load, ATC-40 (Applied Technology Council 1996) and FEMA-356 (Federal Emergency Management Agency 2000) codes are used.

4. The method of model analysis

In order to investigate on the hysteresis behavior of models, nonlinear static analysis is used.

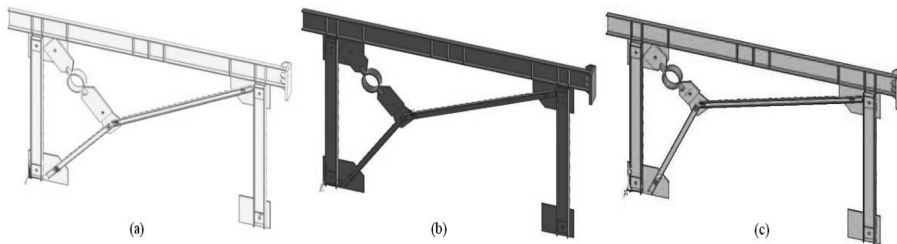


Fig. 2 Hinged frame with off-centre bracing system and ductile element. a) 0.2 eccentricities (Model OBS-C0.2), b) 0.3 eccentricities (Model OBS-C0.3), c) 0.4 eccentricities (Model OBS-C0.4)

Table 1 Sections specification of hinged frame with off-centre bracing system and ductile element

Specification	Members	Column	Beam	Brace OB	Brace OC
Common in all models	Kind of profile	2UNP14	IPE22	2UNP6	2UNP6
	A (mm ²)	4080	3950	1292	1292
	I _x (mm ⁴)	12100000	30600000	632000	632000
	I _y (mm ⁴)	4339500	1620000	561500	561500
	r _x (mm)	54.5	88	22.1	22.1
	r _y (mm)	32.6	20.2	20.8	20.8
Model OBS-C0.2	l (mm)	1500	2750	1800	950
Model OBS-C0.3	l (mm)	1500	2750	1830	980
Model OBS-C0.4	l (mm)	1500	2750	1890	1070

Concerning all above-mentioned reasons, at the end of numerical analysis, Eigen Buckling analysis is conducted to investigate on the braces members buckling and in order to prove the accuracy of modeling.

5. Validation of numerical analysis with experimental data

To validate analytical results, steel ring is considered as a ductile element and for simplification has been named (CT20_TH12_C). Attention to modeling in the International Institute Earthquake Engineering and Seismology (Kafi 2008) another ring with external diameter 220 mm, thickness 12 mm and length of 100 mm with two connections plate $200 \times 170 \times 12$ mm with 7 mm fillet weld is taken, as shown in Fig. 5.

As shown in Fig. 6, the achieved hysteresis plots of experimental and analytical data showed very good superposition.

6. Cyclic load

The load is reciprocating, so it is so similar to earthquakes loads. The method of loading is according to proposed method of ATC_40 code. In the Fig. 7 loading history of ATC_40 code is shown. In this

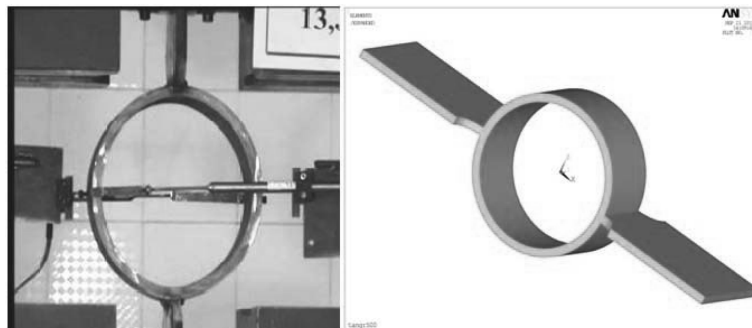


Fig. 5 General view of steel ring in universal jack and ANSYS software

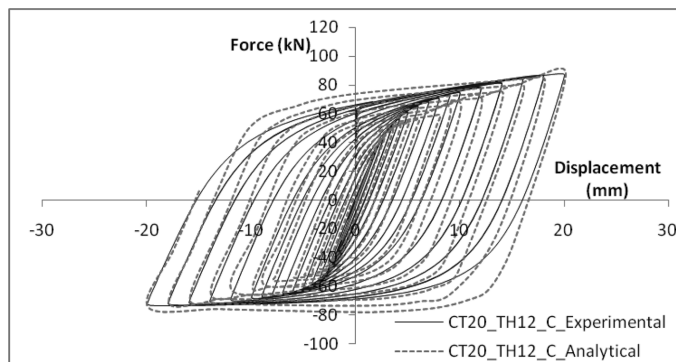


Fig. 6 Comparative hysteresis plots of experimental and analytical results for CT20_TH12_C

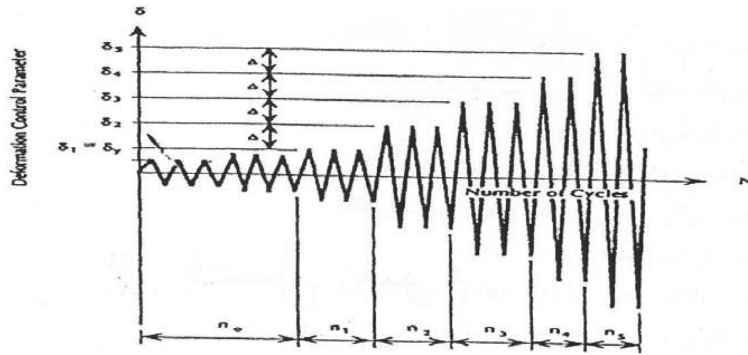


Fig. 7 Loading history in ATC_40 code

figure:

- δ_i : Maximum displacement of loading
- n_i : Number of cycles with δ_i displacement amplitude
- Δ : Yielding displacement of damper

Considering ATC_40 code, loading history of models is shown in Fig. 8 and Table 2.

6.1 Model OBS-C-0.2

The results from the cyclic load analysis of model as force-displacement plot are shown in Fig. 9. This curve continued to ultimate yielding strain of applied steels. To investigate inelastic behavior, the Von Misses yield surface is used. In this analysis, tolerable tensile load in nonlinear limit zone is 222.81 kN and tolerable compressive load in nonlinear limit zone is 225.36 kN. The maximum displacement in nonlinear zone is achieved 32.2 mm.

The obtained hysteresis loops is wide and revealed suitable absorption of input energy to the structure. As shown in Fig. 10, the hysteresis loops push force-displacement plot for frame has been obtained. The maximum tolerable tension load in this system is 222.81 kN and maximum displacement is 32.2 mm and displacement of system at the end of elastic limit is 8.01 mm. The ductility factor (μ) of this system for tension load is

$$\mu = \frac{\Delta_{Max}}{\Delta_y} = \frac{32.2}{8.01} = 4.02 \tag{1}$$

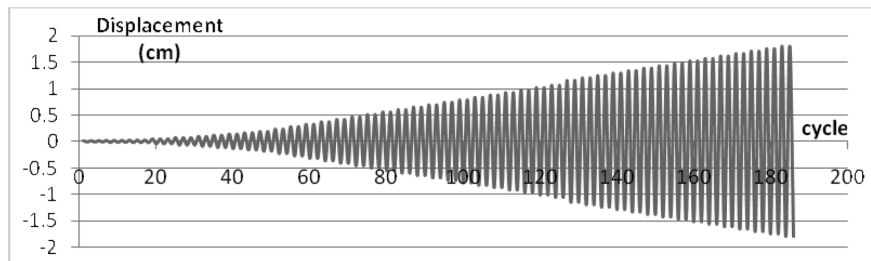


Fig. 8 Loading history of models in this paper

Table 2 Loading history of models in this paper

Cycles	Displacement (mm)		Cycles	Displacement (mm)		Cycles	Displacement (mm)	
Cycle 1	0.115	-0.115	Cycle 16	4.6	-4.6	Cycle 31	11.5	-11.5
Cycle 2	0.1725	-0.1725	Cycle 17	5.06	-5.06	Cycle 32	11.96	-11.96
Cycle 3	0.23	-0.23	Cycle 18	5.52	-5.52	Cycle 33	12.42	-12.42
Cycle 4	0.46	-0.46	Cycle 19	5.98	-5.98	Cycle 34	12.88	-12.88
Cycle 5	0.69	-0.69	Cycle 20	6.44	-6.44	Cycle 35	13.34	-13.34
Cycle 6	0.92	-0.92	Cycle 21	6.9	-6.9	Cycle 36	13.8	-13.8
Cycle 7	1.15	-1.15	Cycle 22	7.36	-7.36	Cycle 37	14.26	-14.26
Cycle 8	1.38	-1.38	Cycle 23	7.82	-7.82	Cycle 38	14.72	-14.72
Cycle 9	1.61	-1.61	Cycle 24	8.28	-8.28	Cycle 39	15.18	-15.18
Cycle 10	1.84	-1.84	Cycle 25	8.74	-8.74	Cycle 40	15.64	-15.64
Cycle 11	2.3	-2.3	Cycle 26	9.2	-9.2	Cycle 41	16.1	-16.1
Cycle 12	2.76	-2.76	Cycle 27	9.66	-9.66	Cycle 42	16.56	-16.56
Cycle 13	3.22	-3.22	Cycle 28	10.12	-10.12	Cycle 43	17.02	-17.02
Cycle 14	3.68	-3.68	Cycle 29	10.58	-10.58	Cycle 44	17.48	-17.48
Cycle 15	4.14	-4.14	Cycle 30	11.04	-11.04	Cycle 45	17.94	-17.94

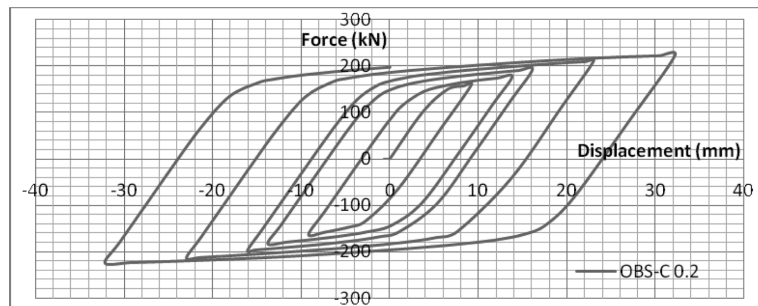


Fig. 9 Force-Lateral displacement plot for Model OBS-C0.2

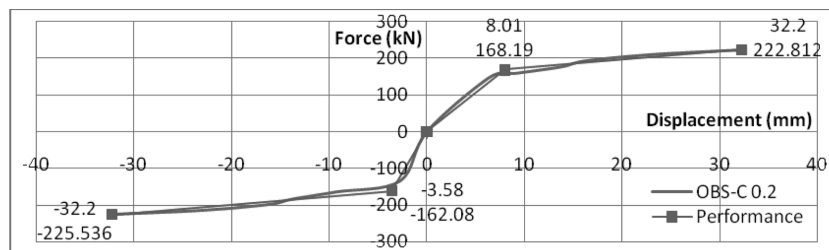


Fig. 10 Hysteresis loops push of force-displacement plot for Model OBS-C0.2

Fig. 11 shows Von Misses stress distribution and Von Misses strain distribution of hinged frame with off-centre bracing system and ductile element. To specify analytical results, the results of investigation on the loading cycles are shown in Table 3.

In Fig. 12 energy-loading cycle plot and in Fig. 13 force-loading cycle plot for hinged frame with off-

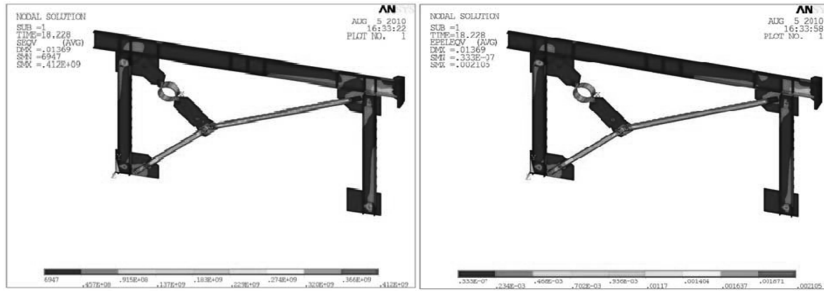


Fig. 11 Von Mises strain and stress under cyclic load for Model OBS-C0.2

Table 3. Analytical results of three models

Models	E_{P-max} (Joule)	E_{E-max} (Joule)	P_{P-max} (kN)	P_{E-max} (kN)	$\frac{E_{P-max}}{E_{E-max}}$	$\frac{P_{P-max}}{P_{E-max}}$	$\frac{(\frac{E_P}{E_E})_{max}}{(\frac{P_P}{P_E})_{max}}$
Model OBS-C0.2	17232.8	41.76	222.812	148.78	412.6	1.5	275.07
Model OBS-C0.3	17414.53	19.28	206.3	72.37	903.24	2.851	316.82
Model OBS-C0.4	8362.57	48.44	114.38	56.43	172.64	2.03	85.04

E_{P-max} : Energy value in the last nonlinear cycle
 E_{E-max} : Energy value in the last linear cycle
 P_{P-max} : Force value in the last nonlinear cycle
 P_{E-max} : Force value in the last linear cycle
 $\frac{E_{P-max}}{E_{E-max}}$: The ratio of energy in the last nonlinear cycle to energy in the last linear cycle
 $\frac{P_{P-max}}{P_{E-max}}$: The ratio of force in the last nonlinear cycle to force in the last linear cycle

centre bracing system and ductile element are shown. Force-energy plot is shown in Fig. 14. As shown in Fig. 14, the high absorption of energy increases by ductile element while the minimum variation of load is applied.

Figs. 15 and 16 respectively have shown displacement-loading cycle plot and cumulative energy-

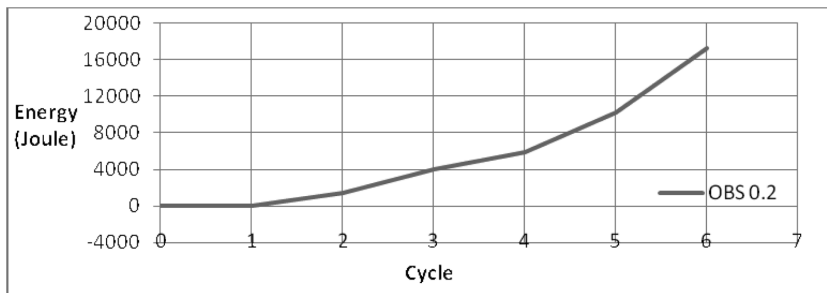


Fig. 12 Energy-Loading cycle plot for Model OBS-C0.2

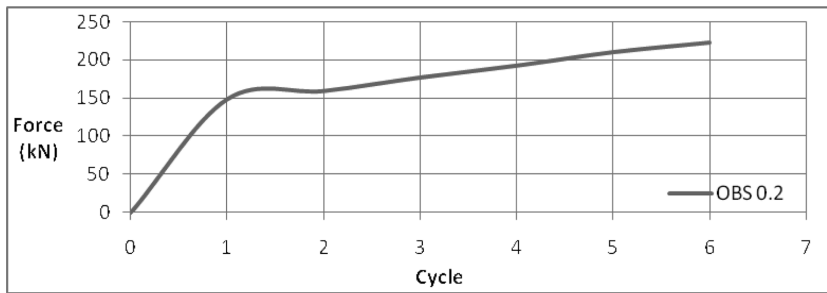


Fig. 13 Force-Loading cycle plot for Model OBS-C0.2

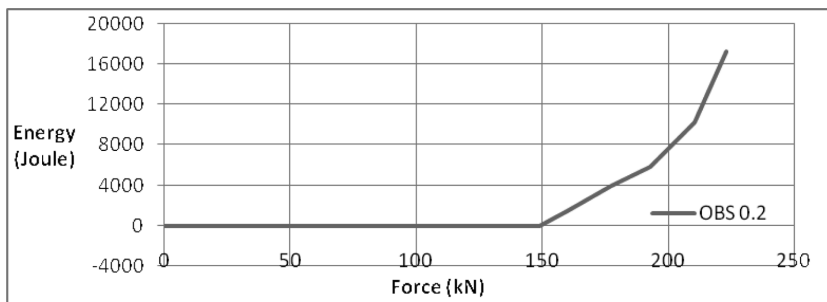


Fig. 14 Force-Energy plot for Model OBS-C0.2

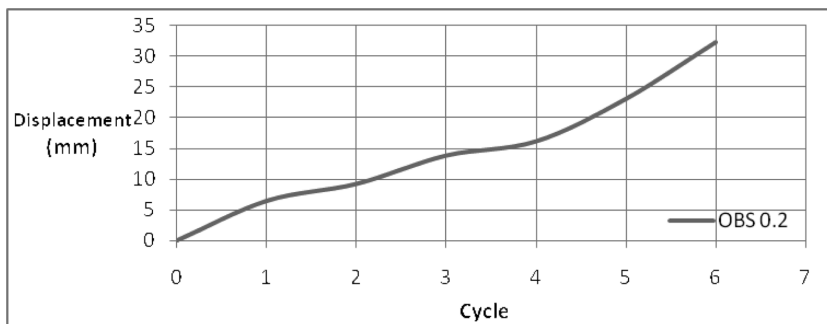


Fig. 15 Lateral Displacement-Loading cycles plot for Model OBS-C0.2

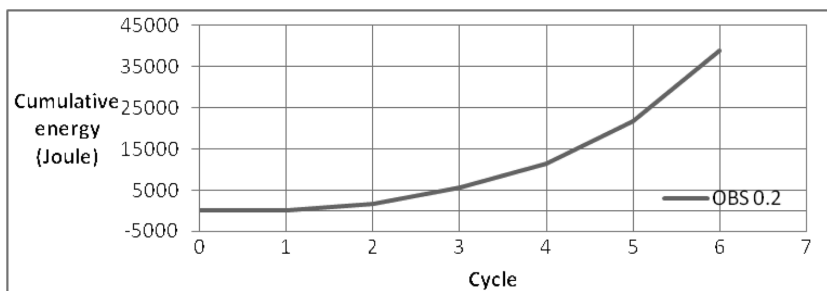


Fig. 16 Cumulative Energy-Loading cycle plot for Model OBS-C0.2

Table 4. Analytical results obtained by force-energy and force-loading cycle plots

Models	Model OBS-C0.2	Model OBS-C0.3	Model OBS-C0.4
Δ_{P-max} (mm)	32.2	36.8	41.4
Δ_{E-max} (mm)	6.44	4.6	9.2
$\sum_{i=1}^n E_i$ (Joule)	38791.25	119375.40	16442.5
$\sum_{i=1}^m E_i$ (Joule)	41.75	86.07	48.44
$\frac{(\Delta_{P-max} - \Delta_{E-max})}{\Delta_{E-max}}$	4	7	3.5
$\bar{E}_p = \frac{(\sum_{i=1}^n E_i - \sum_{i=1}^m E_i)}{(n - m)}$ (Joule)	7749.9	5680.44	3278.81
$\bar{E}_E = \frac{\sum_{i=1}^m E_i}{m}$ (Joule)	41.75	22.74	48.44
$\frac{\bar{E}_p}{\bar{E}_E}$	185.63	249.79	67.69

Δ_{P-max} : Lateral displacement of frame in the last nonlinear cycle

Δ_{E-max} : Lateral displacement of frame in the last linear cycle

$\sum_{i=1}^m E_i$: Total energy in 6 loading cycle

$\sum_{i=1}^n E_i$: Total energy in 1 loading cycle

$\frac{(\Delta_{P-max} - \Delta_{E-max})}{\Delta_{E-max}}$: The ratio of nonlinear lateral displacement to Linear lateral displacement

$\bar{E}_p = \frac{(\sum_{i=1}^m E_i - \sum_{i=1}^n E_i)}{(m - n)}$: Average energy per loading cycle in nonlinear limit zone

$\bar{E}_E = \frac{\sum_{i=1}^n E_i}{n}$: Average energy per loading cycle in linear limit zone

$\frac{\bar{E}_p}{\bar{E}_E}$: The ratio of average nonlinear energy to average linear energy per loading cycle

loading cycle plot for hinged frame with off-centre bracing system and ductile element. The obtained results of these three models are shown in Table 4.

As it is seen, average energy per loading cycle in nonlinear limit zone is 185.63 times the average energy per loading cycle linear limit zone and lateral nonlinear displacement of frame is 4 times more than lateral linear displacement of it. Bearing capacity of frame in nonlinear limit is 1.5 times than the bearing capacity of it in linear limit. Average energy per loading cycle in nonlinear limit is 185.63 times than average energy of it in linear limit.

6.2 Model OBS-C-0.3

The results from the analysis of model under cyclic load as a plot of force-displacement are shown in Fig. 17. This curve continued to ultimate yielding strain of applied steels. To investigate inelastic behavior, The Von Misses yield surface has been utilized. In this analysis, tolerable load in nonlinear limit zone is 206.31 kN and the maximum displacement in nonlinear zone is achieved 36.8 mm.

The obtained hysteresis plot is very wide and revealed suitable absorption of input energy to the structure. As shown in Fig. 18, the hysteresis push force-displacement plot of frame has been obtained. The maximum tolerable load in this system is 206.31 kN and maximum displacement is 36.8 mm and

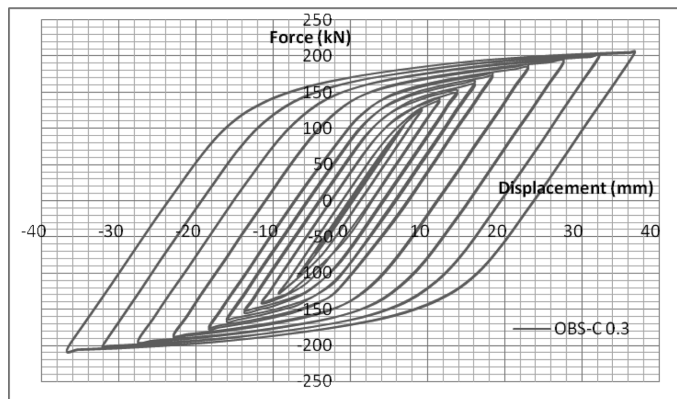


Fig. 17 Force-Lateral displacement plot for Model OBS-C0.3

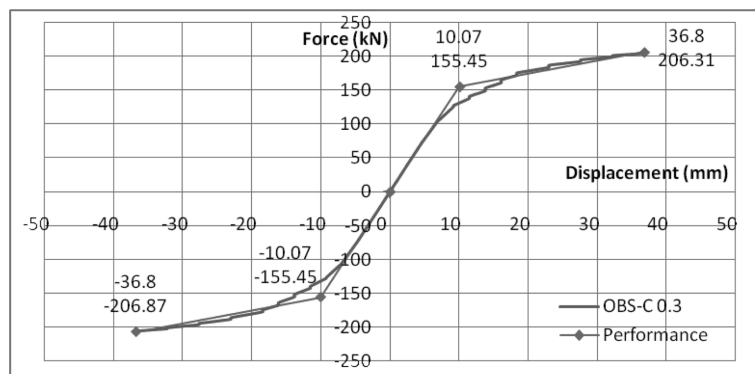


Fig. 18 Hysteresis loops push of force-displacement plot for Model OBS-C0.3

displacement of system at the end of elastic limit is 10 mm. The ductility factor (μ) of this system is

$$\mu = \frac{\Delta_{Max}}{\Delta_y} = \frac{36.8}{10} = 3.7 \tag{2}$$

In Fig. 19 Von Misses stress distribution, Von Misses strain distribution of hinged frame with off-centre bracing system and ductile element are shown.

In Fig. 20 energy-loading cycle plot and in Fig. 21 force-loading cycle plot of hinged frame with off-centre bracing system and ductile element are shown. As it is seen, nonlinear bearing capacity of frame is 2.85 times than the linear bearing capacity of it and the energy of last nonlinear cycle is 903.24 times more than the energy in last linear cycle. In other words, the absorption of energy in the last nonlinear cycle to related force is 316.82 times of absorption of energy in the last linear cycle to related force of it.

Force-energy plot is shown in Fig. 22. As load increases, the gradient of curve increases and in the

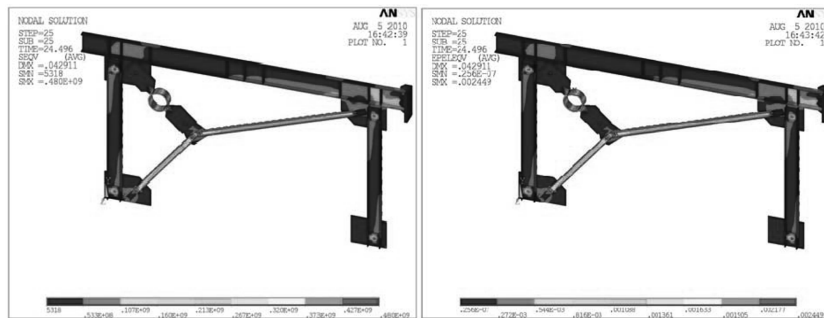


Fig. 19 Von Misses strain and stress under cyclic load for Model OBS-C0.3

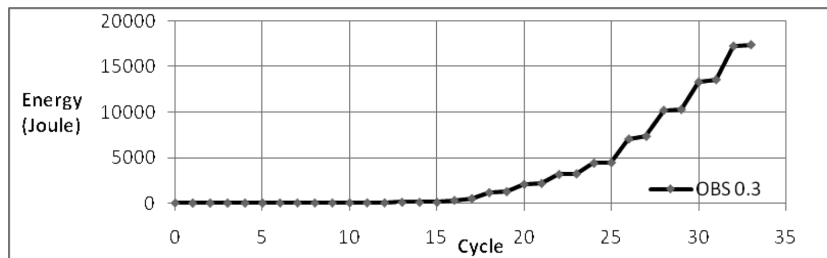


Fig. 20 Energy-Loading cycle plot for Model OBS-C0.3

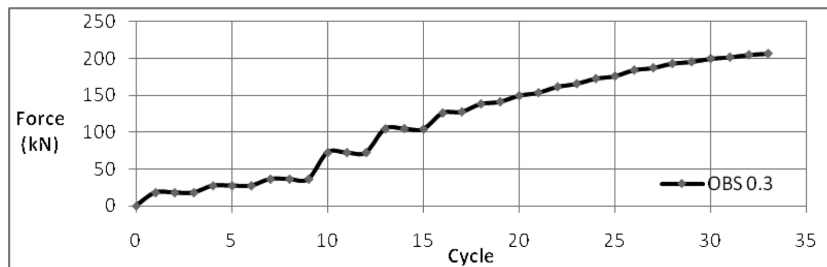


Fig. 21 Force-Loading cycle plot for Model OBS-C0.3

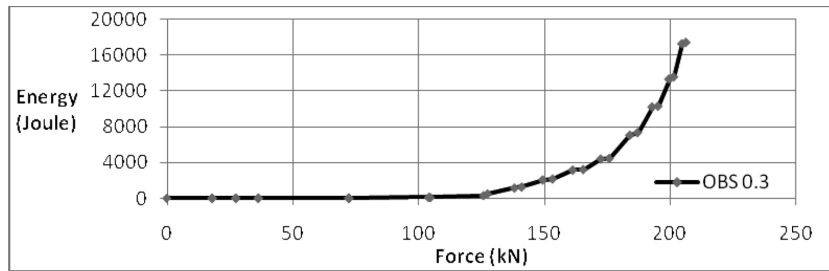


Fig. 22 Force-Energy plot for Model OBS-C0.3

last step of loading, curve gradient approximately reaches to gradient of vertical line. This applies the increase in extremely high energy absorption to the minimum variation of load.

Figs. 23 and 24 respectively have shown displacement-loading cycle plot and cumulative energy-loading cycle plot of hinged frame with off-centre bracing frame and ductile element. As it is seen, average energy per loading cycle in nonlinear limit zone is 249.79 times than the average energy per loading cycle linear limit zone and lateral nonlinear displacement of frame is 7 times more than lateral linear displacement of it. Bearing capacity of frame in nonlinear limit is 2.85 times than bearing capacity of it in linear limit. Average energy per loading cycle in nonlinear limit is 249.79 times of average energy of it in linear limit. The results revealed high energy dissipation in this system. The analytical results from these plots are shown in Tables 3, 4.

6.3 Model OBS-C-0.4

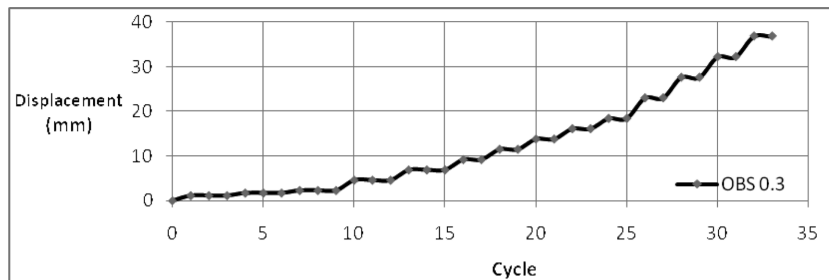


Fig. 23 Lateral displacement-Loading cycles plot for model OBS-C0.3

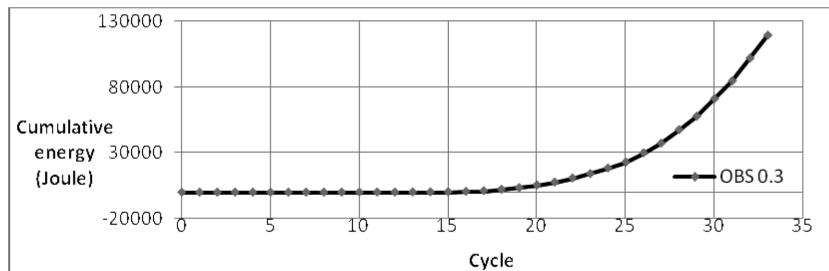


Fig. 24 Cumulative Energy-Loading cycle plot for model OBS-C0.3

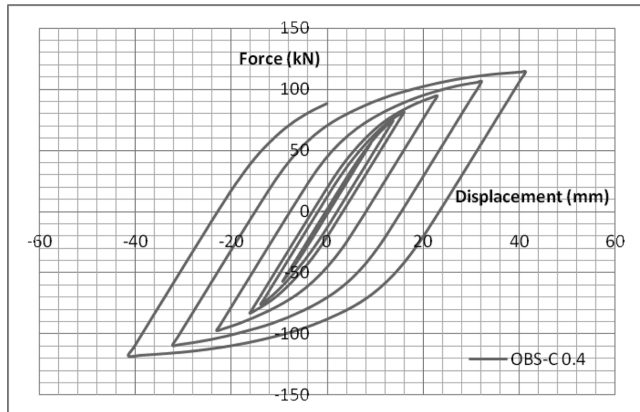


Fig. 25 Force-Displacement plot for Model OBS-C0.4

The results from the analysis of model under cyclic load as plot of force-displacement are shown in Fig. 25. This curve continued to ultimate yielding strain of applied steels. To investigate inelastic behavior, the Von Mises yield surface is used. In this analysis, tolerable tensile load in nonlinear limit zone is 114.38 kN and tolerable compressive load in nonlinear limit zone is 117.78 kN. The maximum displacement in nonlinear zone is achieved 41.4 mm.

The obtained hysteresis plot is wide and revealed suitable absorption of input energy to the structure. As shown in Fig. 26, the hysteresis push force-displacement plot for frame has been obtained. The maximum tolerable load in this system is 114.38 kN and maximum displacement is 41.4 mm and displacement of system at the end of elastic limit is 12.99 mm. The ductility factor (μ) of this system is

$$\mu = \frac{\Delta_{Max}}{\Delta_y} = \frac{41.4}{12.99} = 3.19 \tag{3}$$

In Fig. 27 Von Mises stress distribution, Von Mises strain distribution of hinged frame with off-centre bracing system and ductile element is shown.

In Fig. 28 energy-loading cycle plot and in Fig. 29 force-loading cycle plot of hinged frame with off-centre bracing system and ductile element are shown. As it is seen, nonlinear bearing capacity of frame is 2.03 times than the linear bearing capacity of it and the energy of last nonlinear cycle is 172.64 times more than the energy in last linear cycle. In other words, the absorption of energy in the last nonlinear

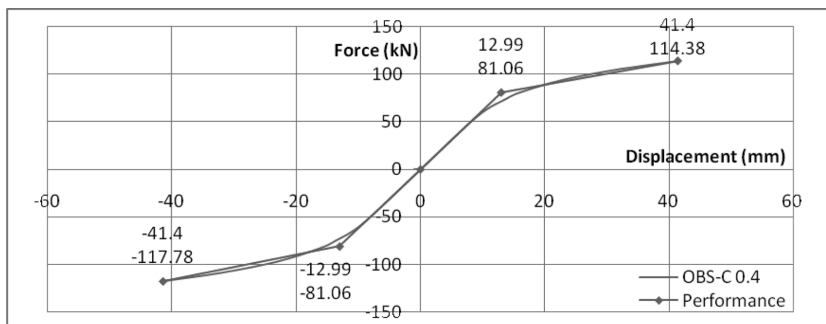


Fig. 26 Hysteresis loops push of force-displacement plot for model OBS-C0.4

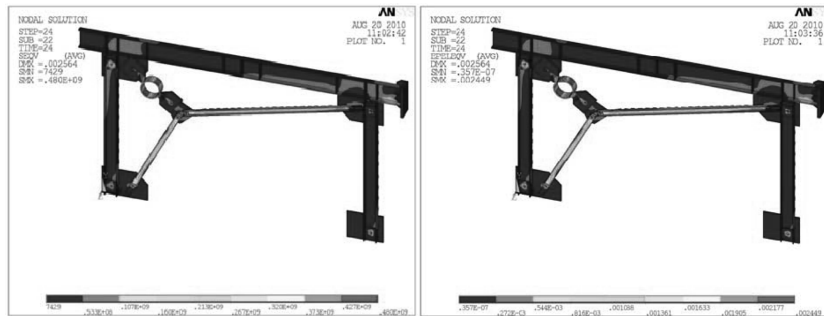


Fig. 27 Von Misses strain and stress under cyclic load for model OBS-C0.4

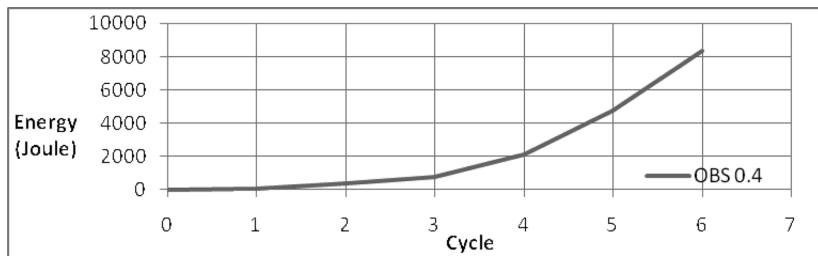


Fig. 28 Energy-Loading cycle plot for model OBS-C0.4

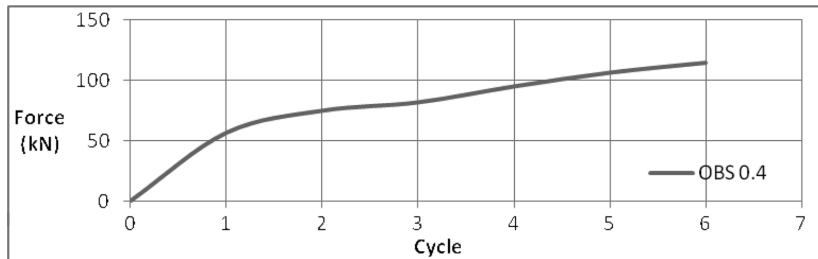


Fig. 29 Force-Loading cycle plot for model OBS-C0.4

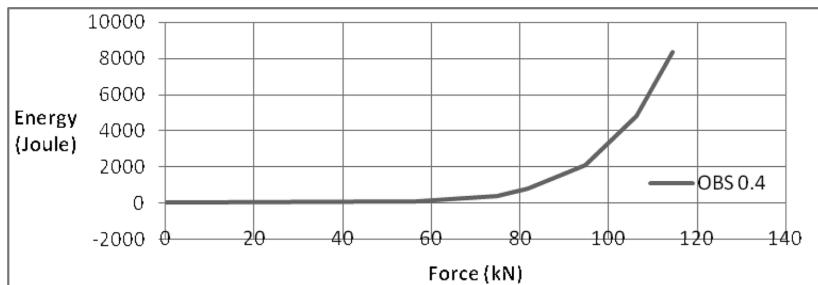


Fig. 30 Force-Energy plot for model OBS-C0.4

cycle to related force is 85.04 times than the absorption of energy in the last linear cycle to related force of it. Force-energy plot is shown in Fig. 30.

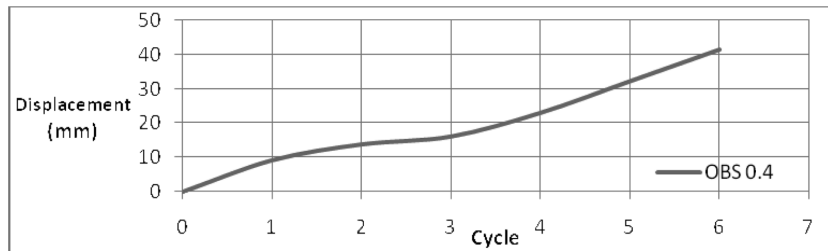


Fig. 31 Lateral displacement-Loading cycles plot for model OBS-C0.4

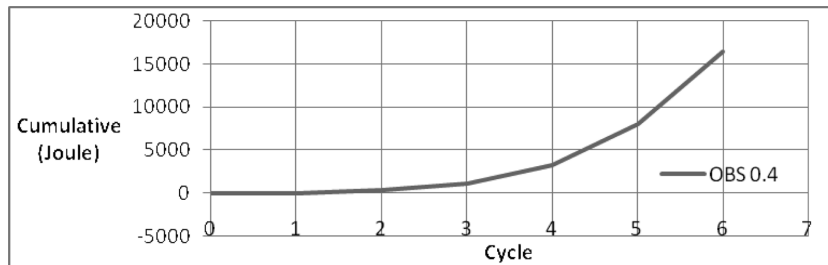


Fig. 32 Cumulative Energy-Loading cycle plot for model OBS-C0.4

Figs. 31 and 32 respectively have shown displacement-loading cycle plot and cumulative energy-loading cycle plot of hinged frame with off-centre bracing frame and ductile element. As it is seen, average energy per loading cycle in nonlinear limit zone is 67.69 times than the average energy per loading cycle linear limit zone and lateral nonlinear displacement of frame is 3.5 times more than the lateral linear displacement of it. Bearing capacity of frame in nonlinear limit is 2.03 times than the bearing capacity of it in linear limit. Average energy per loading cycle in nonlinear limit is 67.69 times than the average energy of it in linear limit.

The analytical results from these plots are shown in Tables 3, 4.

7. Evaluating and comparing the finite element analysis results of models

For more accurate investigation of hysteresis curves, comparing between plots of model OBS-C0.2, OBS-C0.3 and OBS-C0.4 has been done. The most important specifications of them in Figs. 33-37 have been represented. As shown, the results of analysis are restricted to the ultimate strain of steels. In Fig. 33, from hysteresis curve of force-lateral displacement for model OBS-C0.3 the maximum tolerable tensile load in nonlinear limit zone has been obtained 206.31 kN and maximum compressive load in nonlinear limit zone for same model has been obtained 206.87 kN, and also maximum displacement in this model in nonlinear limit zone is 36.8 mm, This value is not maximum displacement of models. Maximum displacement in nonlinear limit zone has been obtained 41.4 mm related to model OBS-C0.4.

As shown in Fig. 34, the value of dissipated energy by off-centre bracing system and ductile element under cyclic load in model OBS-C-0.3 has been obtained 17414.52 joule. It is the maximum dissipated energy value among the models. Model OBS-C-0.4 with 8362.57 joule has a minimum dissipated energy. These values revealed 52% reduction in model OBS-C-0.4 to model OBS-C-0.3, and model OBS-C-0.2 with 17232.8 joule dissipated energy with a reduction percentage of 1.5% to model OBS-C-

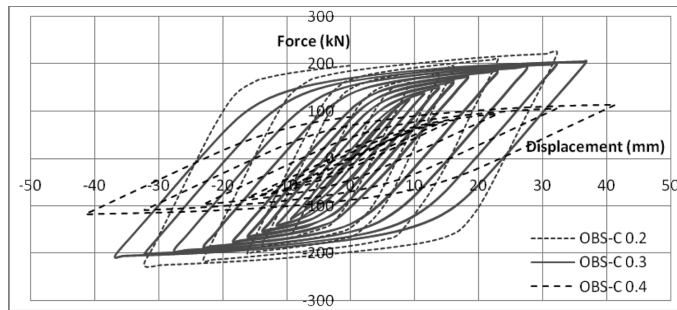


Fig. 33 Comparative hysteresis force-lateral displacement plots for models

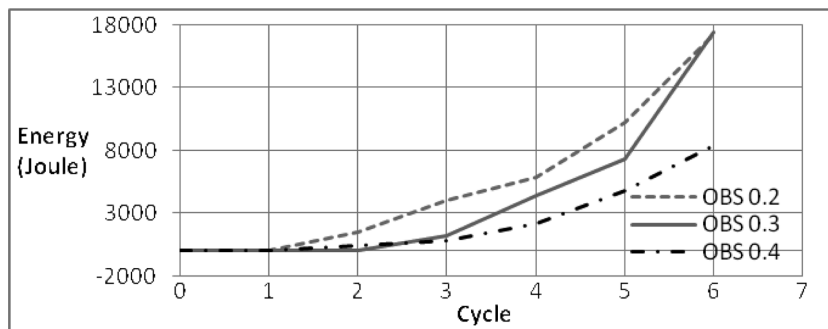


Fig. 34 Comparative energy-loading cycle plots for three models

0.3 and with an increase percentage of 51.47% to model OBS-C-0.4. It must be noted that after preliminary analysis of model OBS-C-0.3 has been considered as an optimum model. Therefore, accuracy of analysis for this model improved significantly. To achieve this purpose, the numbers of loading cycles to analyze this model are more than 5 times than the other ones. This did not created any faults in the ultimate results, so for comparing of these models in the best way 6 main loading cycles of model OBS-C-0.3 have been considered.

As shown in Fig. 35, the value of absorbing force by off-centre bracing system and ductile element under cyclic load in model OBS-C-0.2 has been obtained 222.81 kN. It is the maximum absorbed force value among the models. Model OBS-C-0.4 with 114.38 kN has the minimum absorbed force. These values revealed 48.66% reduction in model OBS-C-0.4 to model OBS-C-0.2, and model OBS-C-0.3 with 206.31 kN absorbed force with a reduction percentage of 7.4% to model OBS-C-0.2 and with an increase percentage of 44.56% to model OBS-C-0.4.

As shown in Fig. 36, comparison between plots of absorbing force-dissipated energy by off-centre bracing system and ductile element under cyclic load revealed that the model OBS-C-0.3 has the maximum absorbed energy while this model transferred less force to structure in comparison with model OBS-C-0.2.

As shown in Fig. 37, lateral displacement of frame in model OBS-C-0.4 has been obtained 41.4mm. This is the maximum value of lateral displacement among the models. Model OBS-C-0.2 with 32.2mm has the minimum lateral displacement .Analysis revealed that model OBS-C-0.4 has 22.22% decrease to model OBS-C-0.2, and lateral displacement of model OBS-C-0.3 with 11% decrease to model OBS-C-0.4 and with 12.5% increase to model OBS-C-0.2 has been obtained 36.8 mm.

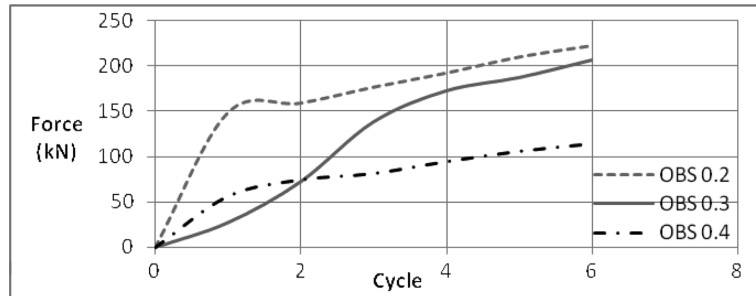


Fig. 35 Comparative force-loading cycle plots for models

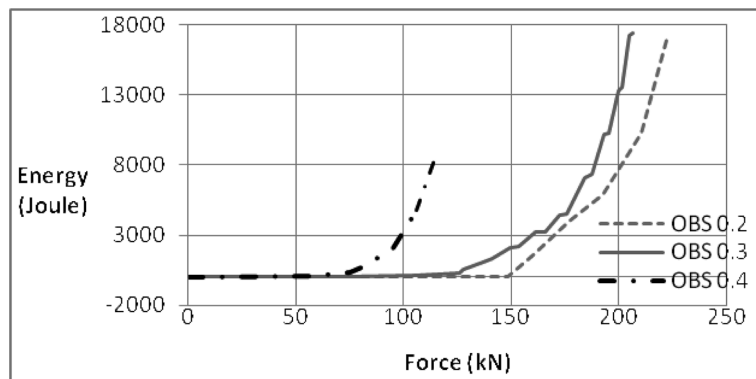


Fig. 36 Comparative force-energy plots for models

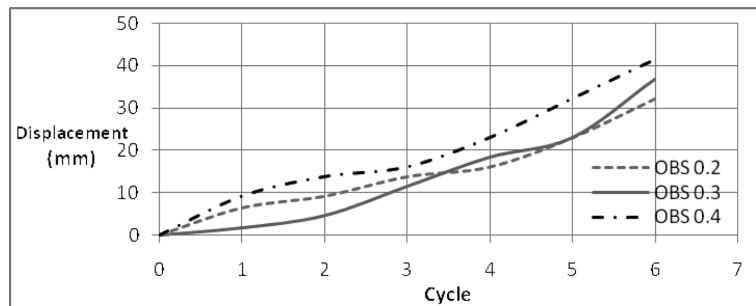


Fig. 37 Comparative lateral displacement-loading cycle plots for models

8. Conclusions

The goal of this paper is to increase the ductility of off-centre braced frame with ductile element, and also to determine the optimum position of ductile element. This bracing has high performance, not needing a special technology and the ability to use steel with available sections and traits in the market. Also Easy replacement of system after damages of hazardous earthquake with low cost and high speed would be available. The new idea of using ductile element in an off-centre bracing would result in these goals. Ductile element built from industrial pipes, and preparing it in order to install in different braces by contractors is performable. Installation of ductile element in bracing system is easy and has low cost.

The results of analysis and investigation on force-displacement behavior of system lead to nonlinear hardening of system. By using ductile element, hardening reduced and in optimum position of ductile element it reached to balance. The increase in displacement of element leads to decrease of displacement for frame and therefore leading to more dissipation of energy in this new system. Considering all reasons like ductility, dissipated energy and etc, analytical results of off-centre bracing system with ductile element model OBS-C-0.2, model OBS-C-0.3 and model OBS-C-0.4 revealed that models OBS-C-0.3 and OBS-C-0.2 have better performance than model OBS-C-0.4. Furthermore models OBS-C-0.3 with 1.5% increase in dissipated energy, 7.4% reduction in tolerable tensile forces, 12.5% increase in displacement and 7.5% reduction in ductility factor in comparison with model OBS-C-0.2 and also constructional point of view model OBS-C-0.3 selected as a system with higher performance in seismic loads. Therefore 0.3 is considered as the best position of ductile element in this research.

Acknowledgments

The first and the forth authors would like to thank the office of gifted students at the Semnan University for Financial Support.

References

- American Institute of Steel Construction (AISC). (2005), "Specification for structural steel buildings", Chicago.
- Andalib, Z., Kafi, M.A. and Bazzaz, M. (2010), "Using hyper elastic material for increasing ductility of bracing", *Proceedings of the 1st. Conference of Steel & Structures and 2nd. Conference on Application of High-Strength Steels in Structural Industry*, Tehran, Iran, December.
- Applied Technology Council (ATC-40). (1996), "Guidelines for cyclic seismic Testing of components of steel structures", ATC. Redwood City USA.
- Bazzaz, M., Kheyroddin, A., Kafi, M.A. and Andalib, Z. (2011), "Evaluating The Performance of Steel Ring in Special Bracing Frame", *Proceedings of the Sixth International Conference of Seismology and Earthquake Engineering*, Tehran, Iran, May.
- Beheshti, A.R. (2008), "Study on increasing capacity bearing of ductile circular element in concentric braces", the degree of Master of Science, Civil Engineering Department, Iran University of Science and Technology, Tehran, Iran, September.
- Building and Housing Research Center. (2007), "Iranian Code of Practice for Seismic Resistant Design of Buildings [Standard No.2800, 3th Edition]", Tehran, Iran.
- Chan Ricky, W.K. and Albermani, F. (2008), "Experimental study of steel slit damper for passive energy dissipation", *J. Eng. Struct.*, **30**(4), 1058-1066.
- Constantinou, M.C., Tsopelas, P., Hammel, W. and Sigaher, A.N. (2001), "Toggle brace-damper seismic energy dissipation systems", *J. Struct. Eng.*, **127**(2), 105-112.
- Federal Emergency Management Agency (FEMA). (2000), "Prestandard and Commentary for the Seismic Rehabilitation of Buildings", Report No. FEMA 356, Washington, USA.
- Hanson, R.D. and Soong, T.T. (2001), "Seismic design with supplemental energy dissipation devices", Oakland (CA): Earthquake Engineering Research Institute.
- Hizji, R. (2008), "Evaluating the performance of concentric braces with preliminary clearance in moment frame", the degree of Master of Science, Civil Engineering Department, Iran University of Science and Technology, Tehran, Iran, September.
- Hsu, H.-L., Juang, J.-L. and Chou, C.-H. (2011), "Experimental evaluation on the seismic performance of steel knee braced frame structures with energy dissipation mechanism", *Steel. Compos. Struct.*, **11**(1), 77-91.

- Ibrahim, Y.E., Marshall, J. and Charney, F.A. (2007), "A visco-plastic device for seismic protection of structures", *J. Constr. Steel. Res.*, **63**, 1515-1528.
- Ibrahim, Y.E. (2005), "A New Visco-Plastic Device for Seismic Protection of Structures", PhD dissertation, Virginia Tech.
- Kafi, M.A. (2008), "Analytical and experimental study of effect of steel ring on ductility of concentric braces", the degree of Doctorate of Philosophy, Civil Engineering Department, Iran University of Science and Technology, Tehran, Iran, September.
- Kafi, M.A. (2008), "Experimental and Analytical Investigation on the Steel Ring Ductility", *Sharif Journal of Science and Technology*, **52**, 41-48.
- Kim, T., Whittaker, A.S., Gilani, A.S.J., Bertero, V.V. and Takhirov, S.M. (2002), "Cover-plate and flangeplate steel moment-resisting connections", *J. Struct. Eng.-ASCE*, **128**(4), 484-482.
- Lee, K. and Bruneau, M. (2005), "Energy dissipation demand of compression members in concentrically braced frames", *Steel. Compos. Struct.*, **5**(5), 345-358.
- Maheri, M.R. and Ghaffarzadeh, H. (2008), "Connection over strength in steel-braced RC frames", *J. Eng. Struct.*, **30**(7), 1938-1948.
- Majidzamani, S., Vafaei, A., Aghakouchak, A.A. and Desai, C. (2011), "Experimental investigation of steel frames braced with symmetrical pairs of y-shaped concentric bracings", *J. Steel Structure*, **11**(2), 117-131.
- Majidzamani, S. and Rasouli, M. (2006), "Experimental investigation of behavior of y-shaped concentric steel bracing", *Asian Journal of Civil Engineering (Building and Housing)*, **7**(1), 81-94.
- Marshall, J.D. and Charney, F.A. (2010), "A hybrid passive control device for steel structures, I: Development and analysis", *J. Constr. Steel. Res.*, **66**(10), 1278-1286.
- Marshall, J.D. and Charney, F.A. (2010), "A hybrid passive control device for steel structures, II: Physical testing", *J. Constr. Steel. Res.*, **66**(10), 1287-1294.
- Moghaddam, H. and Estekanchi, H. (1999), "Seismic behavior of off-centre bracing systems", *J. Constr. Steel. Res.*, **51**(2), 177-196.
- Moghaddam, H. and Estekanchi, H. (1995), "On the characteristics of off-centre bracing system", *J. Constr. Steel. Res.*, **35**(3), 361-376.
- Mualla, I.H. and Belev, B. (2002), "Performance of steel frame with anew friction damper device on the earthquake excitation", *J. Eng. Struct.*, **24**(3), 365-371.
- Murthy, A.N.C.K. (2005), "Application of visco-hyperelastic devices in structural response control", the degree of Master of Science, Civil Engineering Department, Blacksburg Polytechnic Institute, Virginia Polytechnic Institute and State University, 11 May.
- Singh, M.P. and Moreschi, L.M. (2002), "Optimal placement of dampers for passive response control", *Earthq. Eng. Struct. Dynam.*, **31**(4), 955-976.
- Tabatabaei Zavare, M.R.S. (2007), "Investigation on the performance and behavior of a proposed passive damper system in concentric and chevron bracing frames", the degree of Master of Science, Civil Engineering Department, University of Tehran, Tehran, Iran, September.